Activation of the molecular chaperone, sigma 1 receptor, preserves cone function in a murine model of inherited retinal degeneration

Jing Wang[a,b], Alan Saul[b,c], Penny Roon[a], and Sylvia B. Smith[a,b,c,1]

[a]Department of Cellular Biology/Anatomy, Medical College of Georgia, Augusta University, Augusta, GA 30912; [b]James and Jean Culver Vision Discovery Institute, Augusta University, Augusta, GA 30912; and [c]Department of Ophthalmology, Medical College of Georgia, Augusta University, Augusta, GA 30912

Edited by Jeremy Nathans, Johns Hopkins University, Baltimore, MD, and approved May 6, 2016 (received for review November 4, 2015)

Retinal degenerative diseases are major causes of untreatable blindness, and novel approaches to treatment are being sought actively. Here we explored the activation of a unique protein, sigma 1 receptor (Sig1R), in the treatment of PRC loss because of its multifaceted role in cellular survival. We used *Pde6β*^{rd10} (*rd10*) mice, which harbor a mutation in the rod-specific phosphodiesterase gene *Pde6β* and lose rod and cone photoreceptor cells (PRC) within the first 6 wk of life, as a model for severe retinal degeneration. Systemic administration of the high-affinity Sig1R ligand (+)-pentazocine [(+)-PTZ] to *rd10* mice over several weeks led to the rescue of cone function as indicated by electroretinographic recordings using natural noise stimuli and preservation of cone cells upon spectral domain optical coherence tomography and retinal histological examination. The protective effect appears to result from the activation of Sig1R, because *rd10/Sig1R*$^{-/-}$ mice administered (+)-PTZ exhibited no cone preservation. (+)-PTZ treatment was associated with several beneficial cellular phenomena including attenuated reactive gliosis, reduced microglial activation, and decreased oxidative stress in mutant retinas. To our knowledge, this is the first report that activation of Sig1R attenuates inherited PRC loss. The findings may have far-reaching therapeutic implications for retinal neurodegenerative diseases.

photoreceptor | *rd10* mouse | retinal neuroprotection | oxidative stress | (+)-pentazocine

The major cause of untreatable blindness worldwide is retinal degenerative disease. The retinal cells most affected are photoreceptor cells (PRC) and ganglion cells (RGC) (1). PRCs degenerate in retinitis pigmentosa (RP), macular degeneration, and cone-rod dystrophies; RGCs die in glaucoma, optic neuropathies, and diabetic retinopathy. There is great heterogeneity underlying retinal degenerative diseases. Thousands of mutations in >200 genes have been identified that lead to blindness in humans (2). In developing therapeutic strategies to treat blindness, it may not be practical to target each genetic defect; however targeting common disease mechanisms holds promise for the development of realistic treatment for patients suffering from retinal disease. Pathogenic features common to retinal diseases, i.e., oxidative damage, endoplasmic reticulum (ER) stress, inflammation, and apoptosis (3–5), are implicated in neurodegenerative diseases.

Sigma 1 receptor (Sig-1R), a promising target for the treatment of neurodegenerative disease because of its multifaceted roles in cellular survival (6–8), is a unique membrane protein with no homology to other mammalian proteins (9, 10). *N*,*N*-dimethyltryptamine is the only endogenous Sig1R ligand identified (11). Sig1R is bound to ceramide-enriched microdomains in complex with the binding protein/glucose regulated protein 78 (GRP78/BiP) protein and functions as an ER chaperone involved in Ca^{2+} mobilization (12). It regulates neuronal nitric oxide synthase, prevents apoptotic neuronal cell death (13, 14), and modulates the activity of pleiotropic transcription factors including NFκB (15, 16), properties relevant to retinal disease. In vitro and in vivo studies demonstrate powerful neuroprotective effects of Sig1R ligands against RGC death (17–21). (+)-Pentazocine [(+)-PTZ], a synthetic, nonnarcotic benzomorphan with very high affinity for Sig1R (K_d: 5.13 nM; B_{max}: 1,146 fmol/mg protein), is used clinically to alleviate pain (22). Ligands for Sig1R modulate ER stress and Ca^{2+} levels in RGCs and retinal Müller glial cells (23–26). Mice lacking Sig1R (*Sig1R*$^{-/-}$) have late-onset retinal degeneration characterized by RGC loss (27) that is worsened by stress such as optic nerve crush or diabetes (28–30). Retinal Müller glial cells isolated from *Sig1R*$^{-/-}$ mice demonstrate elevated endogenous reactive oxygen species (ROS) accompanied by altered antioxidant gene expression (31).

Sig1R ligands suppress ROS production in multiple cell types (23, 32–34) and inhibit inflammatory cytokine release (16, 35). Oxidative stress increases in models of PRC degeneration (36), and antioxidant treatment delays PRC death (4). Oxidative stress leads to increased levels of the transcription factor nuclear factor erythroid-derived 2-like 2 (NRF2), which translocates to the nucleus to up-regulate the expression of detoxifying and antioxidant genes (37, 38). Compelling data from Cepko's laboratory (39) showed that subretinal delivery of *Nrf2* using adeno-associated viral vectors in neonatal mice promoted the survival of PRC in retinal degeneration models.

Whether activation of Sig1R can attenuate inherited PRC loss and preserve retinal function is unknown. Here we asked whether (+)-PTZ would afford protection against PRC degeneration using mice homozygous for retinal degeneration 10 (hereafter *rd10* mice) in which a mutation of phosphodiesterase 6 β (*Pde6β*) reduces phosphodiesterase enzymatic function, leading to increased

Significance

The role of sigma 1 receptor (Sig1R) in rescuing cone photoreceptor function was investigated in *Pde6β*^{rd10} (*rd10*) mice, a model of severe retinal degeneration. Sig1R, a putative molecular chaperone, is implicated in several human neurodegenerative diseases. We administered (+)-pentazocine, a high-affinity Sig1R ligand, to *rd10* mice, which lose rod and subsequently cone photoreceptor cells (PRC) within the first few weeks of life, rendering them completely blind. Regular administration of (+)-pentazocine rescued cone PRC responses, which were markedly preserved and were similar to those in wild-type mice. To our knowledge, this is the first demonstration of significant preservation of retinal function as a consequence of Sig1R activation. The data are highly relevant to potential therapeutic interventions in human retinal disease.

Author contributions: J.W., A.S., and S.B.S. designed research; J.W., A.S., and P.R. performed research; J.W., A.S., and S.B.S. analyzed data; and S.B.S. wrote the paper.

The authors declare no conflict of interest.

This article is a PNAS Direct Submission.

[1]To whom correspondence should be addressed. Email: sbsmith@augusta.edu.

This article contains supporting information online at www.pnas.org/lookup/suppl/doi:10.1073/pnas.1521749113/-/DCSupplemental.

Downloaded by guest on February 24, 2022

cGMP. Rod PRC death peaks at postnatal day (P) 25; only residual vision remains after P30; cone function is barely detectable by P35 (40, 41). We show that regular administration of (+)-PTZ improves cone function dramatically and appears to protect against cone PRC death by modulating oxidative damage and glial activation. To our knowledge, these findings represent the first targeting of this molecular chaperone as a therapeutic strategy for inherited PRC dystrophy.

Results

Sig1R Activation Rescues Cone Function in *rd10* Mice. *rd10* mice administered (+)-PTZ on alternate days beginning at P14 (hereafter *rd10*+PTZ mice) were subjected to comprehensive electroretinogram (ERG) analysis at P35 to assess rod and cone function. Responses were compared with age-matched untreated *rd10* (hereafter, *rd10*-non) and WT mice. Profound effects of (+)-PTZ treatment were observed in cone PRC function. WT mice had robust cone (Fig. 1*A*) and rod (Fig. S1*A*) responses, regardless of the intensity of the light stimulus (contrast). In *rd10*-non mice only weak cone responses were detected and then only to the brightest stimuli (Fig. 1*B*). In contrast, *rd10*+PTZ mice had significantly improved photopic responses as compared with *rd10*-non mice (Fig. 1*C*). The photopic b-wave amplitude in *rd10*+PTZ mice, which improved significantly compared with that in *rd10*-non mice, was approximately half the amplitude in WT mice (Fig. 1*D*). Results are illustrated in Fig. 1*E*, where averaged responses from the highest contrast are superimposed. An even stronger rescue of cone function in *rd10*+PTZ mice was observed by testing animals with a stimulus that changed more slowly in time (Fig. 1*F*). This natural stimulus produced responses in *rd10*+PTZ mice similar in strength to those in WT mice, although with slightly different timing. These impressive results suggest that cone function, especially for natural stimuli, is preserved by regular administration of (+)-PTZ, underscoring the potential of Sig1R activation as a therapeutic target in retinal disease. Scotopic ERGs showed robust a-wave responses in WT mice (Fig. S1*A*) that were nearly undetectable in *rd10*-non and *rd10*+PTZ mice (Fig. S1 *A* and *B*); there was slight, albeit significant, improvement in rod b-wave amplitude in *rd10*+PTZ mice as compared with nontreated mutants (Fig. S1*C*).

Sig1R Activation Preserves Retinal Thickness and Diminishes Retinal Detachment in *rd10* Mice. We monitored the effects of Sig1R activation on *rd10* retinal structure in vivo using spectral domain optical coherence tomography (SD-OCT). Representative images from WT, *rd10*-non, and *rd10*+PTZ mice are shown in Fig. 2 *A–D*. Retinal measurements acquired using Divers software showed that at P21 the total retinal thickness (TRT) was 226.5 ± 10.7 μm in WT mice and was 193.4 ± 14.6 μm in *rd10*-non mice. The TRT in *rd10*+PTZ mice was 209.8 ± 15.9 μm, significantly greater than in *rd10*-non mice (Fig. 2*E*). Even at P42, the TRT of *rd10*+PTZ mice was significantly greater than that of *rd10*-non mice (Fig. 2*F*). In *rd10* mice PRCs die, and the thickness of the retinal outer nuclear layer (ONL) decreases rapidly over several weeks. At P21, the thickness of the ONL in WT mice was ∼70 μm; in *rd10*+PTZ mice it was ∼55 μm, significantly greater than in *rd10*-non mice (∼45 μm) (Fig. 2*G*). Even in advanced PRC degeneration (at P42), *rd10*+PTZ mice showed preservation of ONL thickness (∼7 μm) significantly greater than in *rd10*-non mice (4 μm) (Fig. 2*H*). Retinal detachment figured prominently in *rd10*-non mice (red arrow in Fig. 2*D*, *Center*) but was attenuated in *rd10*+PTZ mice (27.5 ± 9.8 μm vs. 17.5 ± 5.6 μm, respectively).

Sig1R Activation Preserves PRC Nuclei in *rd10* Mice. In retinal histologic sections the WT retina at P42 is well-organized with ∼10–12 rows in the ONL; inner/outer segments are uniform, and outer segments are in close proximity to the retinal pigment epithelium (RPE) (Fig. 3 *A* and *B*). The inner retinal thickness in *rd10*-non mice is similar to that in WT mice (Fig. 3*C*), but the ONL is reduced to a few PRC nuclei (Fig. 3*D*). Inner/outer segments are not discernible in *rd10* retinas at P42; retinal detachment is considerable (Fig. 3*C*, arrows); and inner segments are severely truncated (Fig. 3*D*, arrows). Retinal detachment was much less prevalent in *rd10*+PTZ mice (Fig. 3*E*) than in *rd10*-non mice (Fig. 3*C*). The inner portion of the *rd10*+PTZ retina was similar in thickness to WT retina (and to *rd10*-non retina) (Fig. 3*F*), and *rd10*-PTZ retinas retained two ONL rows (Fig. 3*F*, arrow). Retinal morphometric analysis showed significant cellular preservation in *rd10*+PTZ mice as compared with *rd10*-non mice. The thickness of the TRT and outer plexiform layer (OPL)

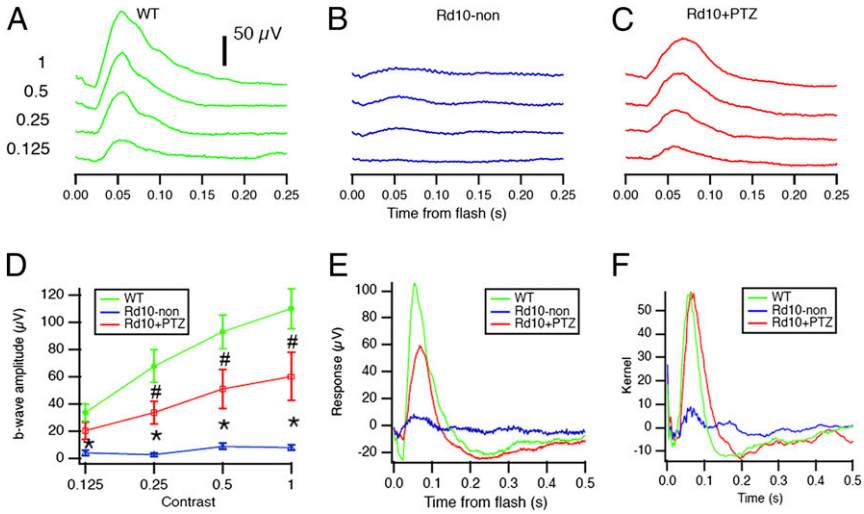

Fig. 1. Photopic ERG responses are improved significantly in *rd10*+PTZ mice. (*A–C*) Averaged photopic responses to 5-ms flashes at a series of intensities (log photopic troland-seconds) are provided for WT (*A*), *rd10*-non (*B*), and *rd10*+PTZ (*C*) mice at P35. (*D*) Mean b-wave amplitudes of averaged photopic responses to 5-ms flashes above a fixed pedestal luminance of 0.105 lumens [four contrasts of the flash; contrast = (flash − pedestal)/pedestal luminance]. Data are the mean ± SEM of four assays using eyes from six to nine mice; *, significantly different from the WT and *rd10*+PTZ groups; #, significantly different from WT and *rd10*-non mice, $P < 0.005$. (*E*) Averaged responses to photopic flash of contrast = 1 (replotted after superimposition). (*F*) Averaged kernels derived from responses to natural noise stimuli. Green, WT mice; blue, *rd10*-non mice; red, *rd10*+PTZ mice. Numbers of mice tested are provided in Table S1.

Downloaded by guest on February 24, 2022

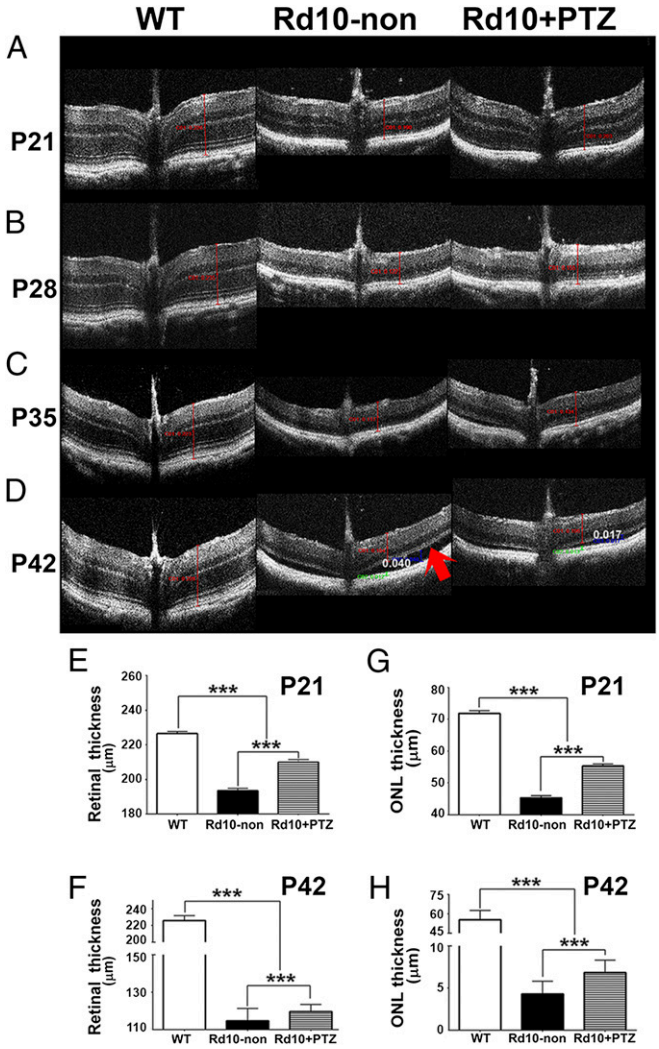

Fig. 2. Improved retinal structure observed in vivo in *rd10*+PTZ mice. (*A–D*) Representative SD-OCT data obtained from WT mice, *rd10*-non mice, and *rd10*+PTZ mice at P21 (*A*), P28 (*B*), P35 (*C*), and P42 (*D*). The arrow in *D* indicates marked retinal detachment. (*E–H*) Data from segmentation analysis for total retinal thickness at P21 (*E*) and P42 (*F*) and for ONL thickness at P21 (*G*) and P42 (*H*). ***$P < 0.001$. Data are the mean ± SEM of analyses in 4–10 mice per group at each age (Table S1).

was greater (Fig. 3 *G* and *H*), there were more rows of nuclei within the ONL (Fig. 3*I*), and the inner segment length was greater (Fig. 3*J*) in *rd10*+PTZ mice than in *rd10*-non mice.

Following PRC degeneration in *rd10* mice, postsynaptic inner nuclear layer (INL) deterioration (rod bipolar and horizontal cell death) ensues (40–42). We asked whether (+)-PTZ treatment attenuated INL cell death in *rd10* mice by evaluating TUNEL$^+$ cells along the horizontal retinal meridian because the degeneration follows a central–peripheral gradient (40). Data for WT, *rd10*-non, *rd10*+PTZ retinas are shown in Fig. S2. WT retinas had few TUNEL$^+$ cells (Fig. S2*A*). Numerous TUNEL$^+$ cells were detected in central, midperipheral, and peripheral regions of the INL of *rd10*-non mice (Fig. S2*B*); whereas *rd10*+PTZ mice had significantly fewer TUNEL$^+$ inner retinal cells than *rd10*-non mice (Fig. S2*C*). Data quantification suggests that (+)-PTZ treatment attenuates secondary INL cell death in this degenerative process (Fig. S2*D*).

Sig1R Activation Attenuates Cone PRC Death in *rd10* Mice. Given the robust photopic response observed in *rd10*+PTZ mice (Fig. 1), we predicted greater cone labeling in *rd10*+PTZ retinas than in *rd10*-non retinas. Immunolabeling of retinal cryosections with anti-cone arrestin antibody supported that prediction and was robust in *rd10*+PTZ retinas as compared with *rd10*-non retinas (Fig. 4 *A–C*). Quantification of fluorescent intensity shows significantly greater cone-arrestin levels in *rd10*+PTZ retinas than in *rd10*-non retinas (Fig. 4*D*). We confirmed these data in retinal cryosections and flatmount preparations using FITC-conjugated peanut agglutinin (PNA), which selectively binds cone inner/outer segments. PNA labeling was uniform in WT retinas (Fig. 4 *E* and *F*) but was reduced significantly in sections of *rd10*-non retinas (Fig. 4 *G* and *H*). Cryosections of *rd10*+PTZ retinas showed labeling of cones in close proximity to cell soma (Fig. 4 *I* and *J*). Immunofluorescence quantification showed that PNA labeling was markedly decreased in *rd10*-non retinas compared with WT retinas but increased significantly in *rd10*+PTZ retinas

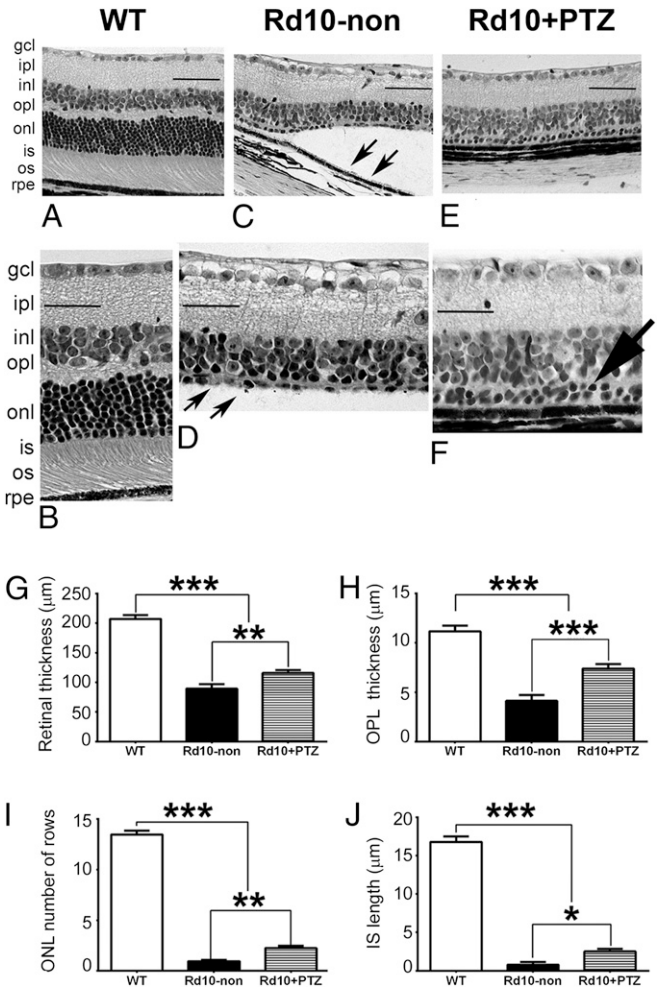

Fig. 3. PRCs are preserved in retinas of *rd10*-PTZ mice. (*A–F*) Retinal sections of eyes embedded in JB-4 and stained with H&E from WT (*A* and *B*), *rd10*-non (*C* and *D*), and *rd10*+PTZ (*E* and *F*) mice. Note retinal detachment (arrows in *C*) and paucity of PRC in the ONL in *rd10*-non mice (arrows in *D*). In *F* two rows of PRC nuclei remain in the ONL of *rd10*+PTZ mice (large arrow). (*G–J*) Morphometric analyses of total retinal thickness (*G*), OPL thickness (*H*), ONL thickness, number of ONL rows (*I*), and inner segment thickness (*J*). gcl, ganglion cell layer; ipl, inner plexiform layer; inl, inner nuclear layer; opl, outer plexiform layer; onl, outer nuclear layer; is, inner segment; os, outer segment; rpe, retinal pigment epithelium. Data are the mean ± SEM of measurements from six to nine mice per group (Table S1); *$P < 0.05$; **$P < 0.01$; ***$P < 0.001$. (Scale bar: 50 μm.) Numbers of mice used in the analysis are provided in Table S1.

Downloaded by guest on February 24, 2022

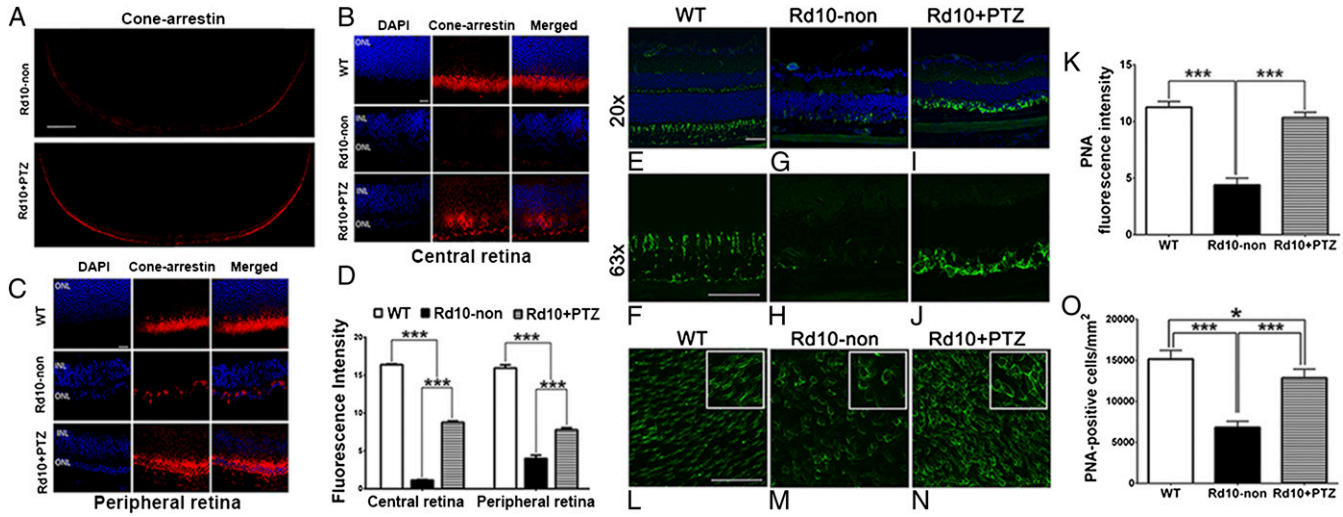

Fig. 4. Many PRCs preserved in *rd10*-PTZ retinas are cones. (*A*) Retinal cross-sections of cone-arrestin labeling in *rd10*-non and *rd10*+PTZ mice. (*B* and *C*) Retinal cryosections subjected to cone-arrestin labeling of the central (*B*) and peripheral (*C*) retina of WT, *rd10*-non, and *rd10*+PTZ mice at P42. (*D*) Quantification of cone-arrestin fluorescence. (*E–J*) Cryosections subjected to PNA immunolabeling from retinas of WT (*E* and *F*), *rd10*–non (*G* and *H*), and *rd10*+PTZ (*I* and *J*) mice at P42. (*K*) Quantification of PNA fluorescence. (*L–N*) Representative PNA-immunolabeled retinal flatmounts from WT (*L*), *rd10*-non (*M*), and *rd10*+PTZ (*N*) mice. (*O*) Quantification of PNA$^+$ cells. Data are the mean ± SEM of three or four assays from six to eight mice (cryosections) and from 7–10 mice (flatmounts) (Table S1). $*P < 0.05$, $***P < 0.001$. (Scale bars: 500 μm in *A*; 20 μm in *B* and *C*; 50 μm in *E–N*.) Nuclei are labeled with DAPI (blue). Numbers of mice used in the analysis are provided in Table S1. Details about antibodies are provided in Table S2.

compared with *rd10*-non retinas (Fig. 4*K*). Immunofluorescence detection of PNA in retinal flatmounts showed intense labeling of WT cone inner segments and soma (Fig. 4*L*). PNA labeling diminished in flatmounts of *rd10*-non retinas (Fig. 4*M*) but was robust in *rd10*+PTZ retinal flatmounts, frequently surrounding cell soma (Fig. 4*N*). Quantification indicated significantly more PNA$^+$ cells in *rd10*+PTZ retinas than in *rd10*-non retinas (Fig. 4*O*). These data showing cone cell preservation in *rd10*+PTZ mice are consistent with the preservation of cone function observed in photopic electrophysiological studies (Fig. 1 *D–F*).

Anti-rhodopsin was abundant in the outer segments of WT retinas (Fig. S3*A*) but diminished markedly in *rd10*-non retinas, localizing only to rudimentary inner segments (Fig. S3*B*). There was slightly more rhodopsin labeling in *rd10*+PTZ retinas than in *rd10*-non retinas (Fig. S3*C*). Quantification of fluorescence showed higher rhodopsin levels in *rd10*+PTZ retinas than in *rd10*-non retinas (Fig. S3*D*), suggesting that rods comprise a small subset of the ONL cells remaining in *rd10*+PTZ retinas.

Sig1R Is Required for Cone Preservation in *rd10* Mice Treated with (+)-PTZ. To determine whether the neuroprotective effects observed with (+)-PTZ treatment in *rd10* mice were caused by Sig1R activation, we generated *rd10* mice lacking *Sig1R* (*rd10*/*Sig1R*$^{-/-}$), treated them with/without (+)-PTZ, and subjected them to ERG, SD-OCT, morphometric analysis, and PNA immunodetection. ERG analysis showed robust photopic responses in WT mice (Fig. 5*A*) but minimal responses in *rd10*/*Sig1R*$^{-/-}$ mice regardless of (+)-PTZ treatment (Fig. 5 *B* and *C*). The amplitude of a-wave and b-wave photopic responses did not differ in *rd10*/*Sig1R*$^{-/-}$ mice, (+)-PTZ–injected (*rd10*/*Sig1R*$^{-/-}$+PTZ) or not (*rd10*/*Sig1R*$^{-/-}$) (Fig. 5 *D* and *E*); amplitudes were reduced markedly compared with those in WT mice. Retinal structure was visualized in vivo using SD-OCT at P21 and P42 (Fig. 5 *F–I*). Segmentation analysis of whole-retinal or ONL thickness showed no significant difference between the two *rd10*/*Sig1R*$^{-/-}$ groups at P21 or P42 (Fig. 5 *J–M*). Eyes were processed for microscopy, and retinas were analyzed morphometrically at P42. The retinas of both *rd10*/*Sig1R*$^{-/-}$-non (Fig. 5 *N* and *O*) and *rd10*/*Sig1R*$^{-/-}$+PTZ (Fig. 5 *P* and *Q*) mice showed marked detachment from RPE and were essentially reduced to the inner retina. They were considerably thinner than the retinas in WT mice (compare Figs. 5 *N–R* and 3 *A*, *B*, and *G*). Only one partial row of nuclei was observed in the ONL of both *rd10*/*Sig1R*$^{-/-}$+PTZ and *rd10*/*Sig1R*$^{-/-}$ mice (Fig. 5 *O* and *Q*). We counted ONL cell bodies (rather than counting rows) and determined there were only ∼10 cells per 100-μm retinal length in either of the *rd10*/*Sig1R*$^{-/-}$ groups (Fig. 5*S*). Flatmount retinal preparations labeled with PNA to detect cones showed abundant labeling in WT retinas (Fig. 5 *T* and *W*) but a paucity of PNA$^+$ cells in *rd10*/*Sig1R*$^{-/-}$ retinas regardless of (+)-PTZ injection (Fig. 5 *U* and *V*). The data indicate that *rd10*/*Sig1R*$^{-/-}$ mice are not afforded PRC neuroprotection when treated with (+)-PTZ, strongly supporting the notion that (+)-PTZ acts through Sig1R to mediate neuroprotection in *rd10* mice.

Sig1R Activation Attenuates Retinal Müller Cell Gliosis and Microglia Activation in *rd10* Mice. In response to pathologic stimuli in retina, Müller radial glial cells become activated (43). This reactive gliosis is considered a cellular attempt to protect tissue from further damage and to promote tissue repair. Reactive gliosis is characterized by increased levels of GFAP, a very sensitive early indicator of retinal stress, in Müller cells (43). WT retinas demonstrated low levels of GFAP with labeling restricted mainly to the nerve fiber layer, typical of astrocyte labeling (Fig. 6*A*). Radial GFAP labeling was intense in *rd10*-non retinas (Fig. 6*B*) but was reduced in *rd10*+PTZ retinas (Fig. 6*C*). Quantitation of intensity showed significantly reduced GFAP levels in *rd10*+PTZ retinas as compared with *rd10*-non retinas (Fig. 6*D*).

Microglial cells are resident retinal immune cells, and microglial reactivity is a hallmark of retinal degenerative and inflammatory diseases, including RP (44). When activated, microglia secrete cytotoxic ROS and nitrogen species, which have deleterious effects on neurons. We prepared whole-retinal flatmounts for immunofluorescence to detect Iba-1, which is up-regulated in activated microglial cells (44). Iba-1 labeling was minimal in WT retinas (Fig. 6*E*) but was abundant in *rd10*-non retinas; the cells in the central and peripheral retina had an amoeboid shape with retracted processes and rounded cell bodies (Fig. 6*F*). In contrast *rd10*+PTZ retinas showed less microglia activation. The central

Downloaded by guest on February 24, 2022

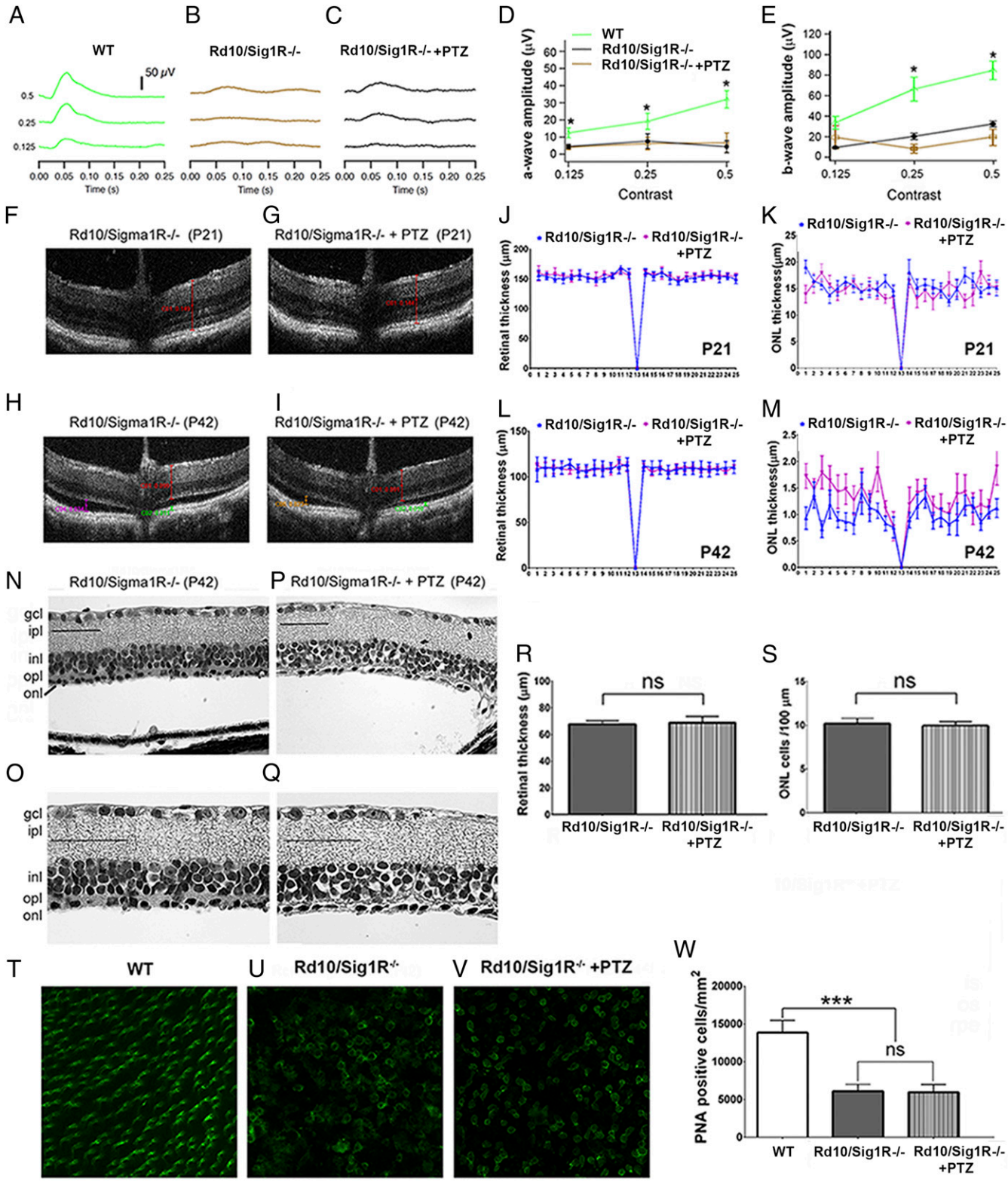

Fig. 5. PRCs are not preserved in *rd10/Sig1R*$^{-/-}$ mice administered (+)-PTZ. (*A*–*C*) ERGs of averaged photopic responses for WT (*A*), *rd10/Sig1R*$^{-/-}$-non (*B*), and *rd10/Sig1R*$^{-/-}$+PTZ (*C*) mice. (*D* and *E*) Mean photopic a-wave (*D*) and b-wave (*E*) amplitudes. *, WT data are significantly different from data from *rd10/Sig1R*$^{-/-}$-non and *rd10/Sig1R*$^{-/-}$+PTZ mice ($P < 0.005$). (*F*–*I*) SD-OCT images of *rd10/Sig1R*$^{-/-}$–non (*F* and *H*) and *rd10/Sig1R*$^{-/-}$-PTZ (*G* and *I*) mice at P21 (*F* and *G*) and P42 (*H* and *I*). (*J*–*M*) Thickness of whole retina (*J* and *L*) and the ONL (*K* and *M*) determined using DIVERS software at P21 (*J* and *K*) and P42 (*L* and *M*). Differences were not significant. (*N*–*Q*) Retinal sections from *rd10/Sig1R*$^{-/-}$-non (*N* and *O*) and *rd10/Sig1R*$^{-/-}$+PTZ (*P* and *Q*) mice. Sections are embedded in JB-4 and stained with H&E. (Scale bars: 50 μm.) For abbreviations see the legend of Fig. 3. (*R* and *S*) Morphometric analysis of retinal thickness (*R*) and the number of ONL cells per100-μm retina length (*S*). (*T*–*V*) PNA immunodetection in retinal flatmounts from WT (*T*), *rd10/Sig1R*$^{-/-}$-non (*U*), and *rd10/Sig1R*$^{-/-}$+PTZ (*V*) mice. (*W*) Quantification of PNA^{+} cells. ***$P < 0.001$; ns, not significant. Numbers of mice used in the analysis are provided Table S1.

Downloaded by guest on February 24, 2022

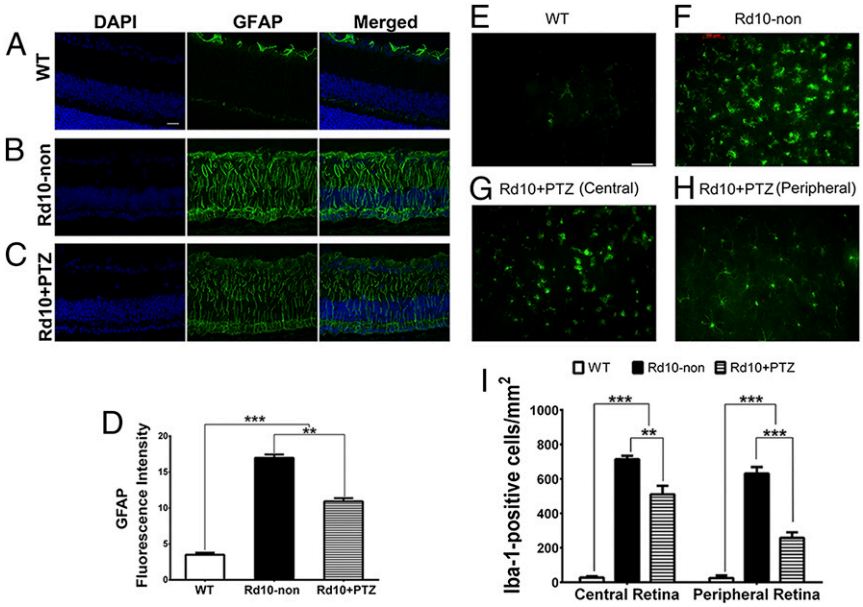

Fig. 6. Müller cell gliosis and microglial activation are attenuated in *rd10*-PTZ mice. (*A*–*C*) Immunodetection of GFAP (green) in retinal cryosections from WT (*A*), *rd10*-non (*B*), and *rd10*+PTZ mice (*C*) at P42. Nuclei are labeled with DAPI (blue). (*D*) Quantitation of fluorescence intensity. (*E* and *F*) Retinal flatmounts from WT (*E*) and *rd10*-non (*F*) mice. (*G* and *H*) Retinal flatmounts immunolabeled with Iba-1 of central (*G*) and peripheral (*H*) retina from *rd10*+PTZ mice. (*I*) Quantitation of fluorescence intensity. Data are the mean ± SEM (three or four assays) from six to eight mice (Table S1). $^{**}P < 0.01$; $^{***}P < 0.001$. (Scale bar: 50 μm.) Details about antibodies are provided in Table S2.

rd10+PTZ retina had fewer activated microglia (Fig. 6*G*). More striking was the *rd10*+PTZ peripheral retina, which showed fewer amoeboid microglia and less microglia infiltration (Fig. 6*H*) than seen in *rd10*-non retinas. Quantification of fluorescence intensity showed significant reduction of Iba-1 labeling in the central and peripheral retina of *rd10*+PTZ retinas (Fig. 6*I*).

Sig1R Activation Attenuates Oxidative Stress in Retinas of *rd10* Mice. Oxidative damage is implicated in PRC death in animal models of RP, including *rd10* mice (45, 46). Administration of (+)-PTZ is protective against ROS accumulation in several retinal cell types (16, 23, 32–34). We investigated whether (+)-PTZ could attenuate oxidative stress in vivo. We quantified retinal lipid oxidation by measuring the level of malondialdehyde (MDA), a byproduct of lipid peroxidation which forms a 1:2 adduct with thiobarbituric acid (TBA), using a commercially available kit. At P42, a baseline level of lipid oxidation was observed in WT retinas; MDA levels were nearly doubled in *rd10*-non retinas as compared with WT retinas but were significantly lower in *rd10*-PTZ retinas than in *rd10*-non retinas (Fig. 7*A*). Retinal protein oxidation was determined by measuring the carbonyl content of proteins using 2,4 dinitrophenylhydrazine (DNPH). At P42, protein carbonylation was reduced significantly in *rd10*+PTZ retinas as compared with *rd10*-non retinas and did not differ significantly from WT retinas (Fig. 7*B*). The data suggest that retinal lipids and proteins undergo oxidative stress in the *rd10* retina and that regular administration of (+)-PTZ attenuates lipid and protein oxidative stress. We investigated further whether (+)-PTZ–mediated effects were associated with decreased oxidation in the retina by subjecting retinal cryosections from WT, *rd10*-non, and *rd10*+PTZ mice to hydroethidine, a dye that emits red fluorescence when it reacts with superoxide radicals. Minimal red fluorescence was observed in WT retinas, but strong red fluorescence was detected in the INL of *rd10*-non retinas. This result is consistent with earlier reports (39, 45). In the retinas of *rd10*+PTZ mice the level of red fluorescence was reduced markedly from that in the retinas of *rd10*-non mice (Fig. 7*C*). Because oxidative stress can increase NRF2 levels, with subsequent up-regulation of antioxidant genes (37), we compared NRF2 levels in WT, *rd10*-non, and *rd10*+PTZ retinas. NRF2 protein levels were significantly higher in *rd10*-non retinas than in WT retinas but were lower in *rd10*+PTZ retinas than in *rd10*-non retinas (Fig. 7 *D* and *E*). The expression of genes encoding the antioxidant proteins superoxide dismutase 1 (*Sod1*), catalase (*Cat*), heme oxygenase 1 (*Hmox1*), and glutathione peroxidase 1 (*Gpx1*) was increased in the retinas of *rd10* mice, consistent with earlier reports (46). Treatment of the *rd10* mice with (+)-PTZ attenuated the increased expression of these antioxidant genes (Fig. 7*F*). Our findings that oxidative stress is a prominent feature of the *rd10* retina are consistent with observations from other laboratories (45, 46), and our data support a role for Sig1R activation in reducing oxidative stress in vivo. Our findings shown in Figs. 6 and 7 suggest that regular administration of (+)-PTZ attenuates reactive gliosis, decreases microglial activation, and decreases oxidative stress in the *rd10* retina.

Discussion

This study examined whether Sig1R activation would afford protection in a model of severe retinal degeneration, the *rd10* mouse, which loses rods and then cones over a 35-d period (40, 41). In human RP patients, rod loss compromises vision in dim light, but it is the later loss of cones that is most debilitating. Cones mediate best vision, and if strategies can be developed that preserve cone function, even when rods are lost, the therapeutic impact on this devastating disease would be enormous.

Our findings offer compelling functional and structural evidence that activation of Sig1R may hold promise as a therapeutic strategy for cone preservation. The functional data show that cone responses in mutant retinas were rescued with regular (+)-PTZ administration. In *rd10*+PTZ mice the photopic b-wave amplitude showed marked improvement from a flat ERG to approximately half the WT amplitude. When natural noise stimuli were presented in ERG testing, cone function improved markedly in *rd10*+PTZ vs. *rd10*-non mice and in *rd10*+PTZ mice was very similar to levels in WT mice. Frequently intervention studies using *rd10* mice compare data for treated animals and nontreated mutants but less often include data for WT mice. In our scenario, cone responses of

Downloaded by guest on February 24, 2022

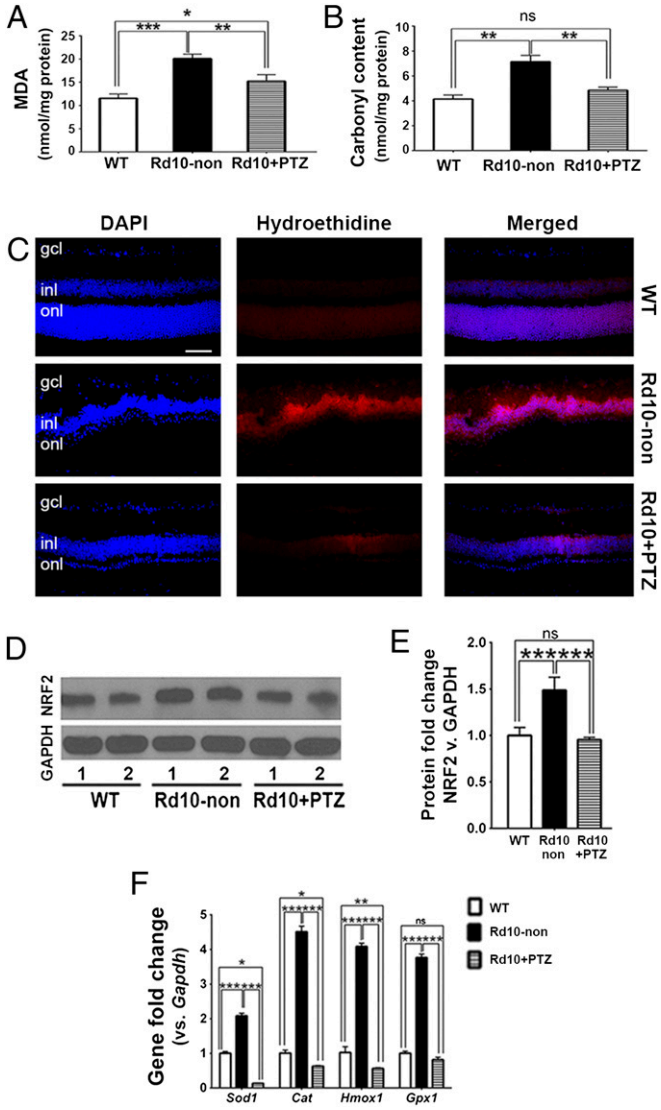

Fig. 7. Oxidative stress is attenuated in *rd10*+PTZ mice. (*A*) Retinal lipid oxidation was quantified as the TBA level by measuring MDA. (*B*) Retinal protein oxidation measured as the carbonyl content of proteins using DNPH in WT, *rd10*-non, and *rd10*+PTZ mice. (*C*) Immunodetection of hydroethidine (red fluorescence upon reaction with superoxide species) in retinal cryosections of WT, *rd10*-non, and *rd10*+PTZ mice at P42. Nuclei are labeled with DAPI (blue). (Scale bar: 50 μm.) (*D*) Neural retinas harvested from WT, *rd10*-non, and *rd10*+PTZ mice at P42 were used for isolation of protein. Representative immunoblots detecting NRF2 are shown. GAPDH was the internal control. Lanes 1 and 2 are two independent samples from different mice. (*E*) Band densities, quantified densitometrically and expressed as fold change vs. GAPDH. (*F*) RNA was isolated from neural retinas and subjected to quantitative real-time RT-PCR analysis of *Sod1*, *Cat*, *Hmox1*, and *Gpx1*. Primer pairs are listed in Table S3. Data are the mean ± SEM of three or four assays. $^{*}P < 0.05$; $^{**}P < 0.01$; $^{***}P < 0.001$.

treated animals are compared not only with those of untreated mutants but also with those of WT mice. There is striking preservation of function with (+)-PZT treatment. SD-OCT showed slight improvement in overall retinal thickness in situ in *rd10*+PTZ mice as compared with *rd10*-non mice, and these observations were borne out by histological investigation. Functional analyses were complemented by the evaluation of retinal sections, and morphometric analyses revealed the preservation of approximately two or three rows of PRC in *rd10*+PTZ mice by P42. Immunolabeling studies indicated that most cells were cones. To our knowledge, our study is the first investigation of Sig1R as a protective agent in a model of inherited PRC degeneration. Recently, Hara's group (47) investigated whether Sig1R activation could protect against PRC loss in a model of intensive light-induced damage by administering the Sig1R ligand cutamesine intravitreally 1 h before light damage. They reported improved retinal function and architecture in this experimental paradigm.

To determine whether (+)-PTZ was neuroprotective through activation of Sig1R, we established a colony of *rd10*/*Sig1R*$^{-/-}$ mice and injected one group with (+)-PTZ. We performed ERG, SD-OCT, morphometric analysis, and immunolabeling of cones. We did not observe cone preservation in any assessments; we conclude that (+)-PTZ–mediated retinal neuroprotection requires Sig1R. These findings are consistent with reports that NMDA-induced RGC death was attenuated in WT mice administered (+)-PTZ but not in mice lacking Sig1R (48).

A question raised by our study is whether (+)-PTZ can prevent or simply delay PRC death. We administered (+)-PTZ from P14 through P42; during this time frame *rd10* mice lose nearly all PRCs. The exciting findings we observed with (+)-PTZ suggest preservation of cone cells, but we do not know whether cone function/viability would continue if (+)-PTZ were administered for many months (or at a higher dosage). Our findings lay the foundation for long-term investigations to address the critical issue of the sustainability of rescue.

In retina, Sig1R mRNA and protein are expressed in RGC, PRC, RPE, and Müller cells (49–51). We do not know which retinal cell type—the degenerating neuron or supportive cells such as Müller cells—is targeted using (+)-PTZ. Earlier in vitro studies demonstrated attenuation of oxidative stress-induced death of isolated RGCs when pretreated with (+)-PTZ, suggesting that the ligand has a direct protective effect on neurons (29). However, (+)-PTZ treatment also can attenuate cytokine release (16) and oxidative stress (31) in isolated Müller cells. Determining which retinal cell type is actually targeted by Sig1R ligands in an in vivo model of retinopathy warrants comprehensive investigation that may involve eliminating Sig1R in specific retinal cell types.

In response to retinal degenerative disease, Müller glial cells undergo reactive gliosis, a cellular strategy thought to protect tissue and promote repair (43). GFAP, an indicator of retinal stress, increased markedly in radially oriented Müller cells in *rd10*-non retinas. Activation of Sig1R decreased GFAP levels significantly in retinas from *rd10*+PTZ mice. Microglial cells also become activated under retinal stress, and levels of the microglial marker Iba-1 were much greater in *rd10* retinas than in WT retinas but were decreased from *rd10*-non levels in *rd10*+PTZ retinas. These findings strongly suggest that Sig1R activation attenuates reactive gliosis and microglial activation.

Oxidative stress, implicated in retinal degeneration, is linked causally with cone death in RP (4, 36, 45). We observed increased oxidized lipids and proteins in *rd10* retinas, which diminished significantly in retinas from *rd10*+PTZ mice. (+)-PTZ treatment of *rd10* mice was associated with decreased superoxide levels in retinal histologic sections. At P42, the *rd10* retina demonstrated elevated levels of NRF2 and increased expression of several antioxidant genes, which were attenuated by (+)-PTZ treatment. The increased expression of antioxidant genes in *rd10* mice as degeneration progresses has been reported earlier (46) and was interpreted as a response to stress. The stress is likely associated with the death of cells in the INL secondary to the devastating PRC death in the ONL (40–42). INL death was confirmed by TUNEL assay (Fig. S2). Increased NRF2 protein levels, as a consequence of oxidative stress, have been reported in vitro. Zhang's laboratory (52) showed that NRF2 levels increased in ARPE-19 cells exposed to cigarette smoke extract; levels were attenuated by treatment with *N*-acetylcysteine, an antioxidant. Understanding whether Sigma1R has a role in modulating antioxidant gene expression and NRF2 levels could be addressed in future studies by crossing *Nrf2*$^{-/-}$ mice with *rd10* mice in the

Downloaded by guest on February 24, 2022

presence/absence of (+)-PTZ treatment. Given the pleiotropic nature of Sig1R ligands (8), it is possible that (+)-PTZ could use several mechanisms to afford protection, but this possibility awaits comprehensive investigation.

The paucity of effective treatments for blinding retinal diseases, coupled with information about new therapeutic targets, has prompted intense investigation of innovative strategies to combat debilitating retinopathies. The *rd10* mouse has proven quite informative in this regard (39, 46, 53–56). Our findings that the activation of Sig1R has powerful neuroprotective effects in this murine model are extremely encouraging. The robust rescue of cone function in *rd10* mice treated with (+)-PTZ appears to be attributable (at least in part) to attenuated Müller cell gliosis, reduced microglial activation, and decreased oxidative stress. Sig1R, whose activation also has been reported to attenuate excitotoxicity (13, 18), calcium dysregulation (12, 17, 26), ER stress (12, 23, 32), and inflammation (15, 16, 35), constitutes a promising target for pharmacologically treating retinal disease.

Material and Methods

Animals and Administration of (+)-PTZ. Three groups of mice were used: WT, *rd10*-non, and *rd10*+PTZ mice. *rd10*+PTZ mice received an i.p. injection of (+)-PTZ (0.5 mg/kg) (Sigma-Aldrich) on alternate days beginning at P14. The dosage was based on studies showing efficacy in attenuating RGC death in diabetic mice (21) and is consistent with safe dosages in humans (57). Additionally, *rd10/Sig1R*$^{-/-}$ were generated and administered (+)-PTZ. Animals were maintained according to the Association for Research in Vision and Ophthalmology statement for the Use of Animals in Ophthalmic and Vision Research. Animals were maintained according to guidelines of the institutional animal care and use committee (IACUC) following our IACUC-approved protocol. Details are provided in *SI Materials and Methods*.

Evaluation of Retinal Phenotype, Cell Death, and Glial Activation. Mice were subjected to functional testing using scotopic and photopic ERGs. Retinal structure was assessed in living animals using SD-OCT. Subsequently, retinas were harvested for morphometric evaluation using fixed, plastic-embedded sections. Retinal cryosections were prepared for immunohistochemical analysis of retinal neuronal and glial cell markers and for analysis of cell death by TUNEL assay. Additional retinas were prepared as flatmounts for immunohistochemical analysis. Details of these experiments are provided in *SI Materials and Methods*.

Evaluation of Oxidative Stress. Retinas were isolated from WT mice, *rd10* mice [injected or not injected with (+)-PTZ], and *rd10/Sig1R*$^{-/-}$ mice and were evaluated for retinal lipid and protein oxidation, levels of hydroethidine, expression levels of antioxidant genes *Sod1*, *Cat*, *Hmox-1*, and *Gpx1*, and NRF2 protein levels. Details are provided in *SI Materials and Methods*.

ACKNOWLEDGMENTS. We thank Dr. Eric Zorrilla, Scripps Research Institute, for providing the initial breeding pairs of *Sig1R*$^{-/-}$ mice. This work was supported by NIH Grant R01 EY014560 and by the James and Jean Culver Vision Discovery Institute. The Electron Microscopy/Histology and the Imaging core facilities of Augusta University provided support for these studies. The Medical College of Georgia provided resources for mouse visual function testing equipment.

1. Dowling JE (2014) Restoring vision to the blind: Introduction. *Transl Vis Sci Technol* 3(7):2.
2. Ran X, et al. (2014) 'RetinoGenetics': A comprehensive mutation database for genes related to inherited retinal degeneration. *Database (Oxford)* 2014:2014.
3. Cuenca N, et al. (2014) Cellular responses following retinal injuries and therapeutic approaches for neurodegenerative diseases. *Prog Retin Eye Res* 43:17–75.
4. Komeima K, Rogers BS, Lu L, Campochiaro PA (2006) Antioxidants reduce cone cell death in a model of retinitis pigmentosa. *Proc Natl Acad Sci USA* 103(30): 11300–11305.
5. Zhang SX, Ma JH, Bhatta M, Fliesler SJ, Wang JJ (2015) The unfolded protein response in retinal vascular diseases: Implications and therapeutic potential beyond protein folding. *Prog Retin Eye Res* 45:111–131.
6. Nguyen L, et al. (2015) Role of sigma-1 receptors in neurodegenerative diseases. *J Pharmacol Sci* 127(1):17–29.
7. Tsai SY, et al. (2009) Sigma-1 receptors regulate hippocampal dendritic spine formation via a free radical-sensitive mechanism involving Rac1xGTP pathway. *Proc Natl Acad Sci USA* 106(52):22468–22473.
8. Ruscher K, Wieloch T (2015) The involvement of the sigma-1 receptor in neurodegeneration and neurorestoration. *J Pharmacol Sci* 127(1):30–35.
9. Brune S, Pricl S, Wünsch B (2013) Structure of the σ1 receptor and its ligand binding site. *J Med Chem* 56(24):9809–9819.
10. Moebius FF, Bermoser K, Reiter RJ, Hanner M, Glossmann H (1996) Yeast sterol C8-C7 isomerase: Identification and characterization of a high-affinity binding site for enzyme inhibitors. *Biochemistry* 35(51):16871–16878.
11. Fontanilla D, et al. (2009) The hallucinogen N,N-dimethyltryptamine (DMT) is an endogenous sigma-1 receptor regulator. *Science* 323(5916):934–937.
12. Hayashi T, Su TP (2003) Sigma-1 receptors (sigma(1) binding sites) form raft-like microdomains and target lipid droplets on the endoplasmic reticulum: Roles in endoplasmic reticulum lipid compartmentalization and export. *J Pharmacol Exp Ther* 306(2):718–725.
13. Griesmaier E, et al. (2012) Neuroprotective effects of the sigma-1 receptor ligand PRE-084 against excitotoxic perinatal brain injury in newborn mice. *Exp Neurol* 237(2): 388–395.
14. Zhang Y, et al. (2012) Sigma-1 receptor agonists provide neuroprotection against gp120 via a change in bcl-2 expression in mouse neuronal cultures. *Brain Res* 1431:13–22.
15. Meunier J, Hayashi T (2010) Sigma-1 receptors regulate Bcl-2 expression by reactive oxygen species-dependent transcriptional regulation of nuclear factor kappaB. *J Pharmacol Exp Ther* 332(2):388–397.
16. Shanmugam A, et al. (2015) Sigma receptor 1 activation attenuates release of inflammatory cytokines MIP1γ, MIP2, MIP3α, and IL12 (p40/p70) by retinal Müller glial cells. *J Neurochem* 132(5):546–558.
17. Tchedre KT, Yorio T (2008) sigma-1 receptors protect RGC-5 cells from apoptosis by regulating intracellular calcium, Bax levels, and caspase-3 activation. *Invest Ophthalmol Vis Sci* 49(6):2577–2588.
18. Martin PM, Ola MS, Agarwal N, Ganapathy V, Smith SB (2004) The sigma receptor ligand (+)-pentazocine prevents apoptotic retinal ganglion cell death induced in vitro by homocysteine and glutamate. *Brain Res Mol Brain Res* 123(1-2):66–75.
19. Dun Y, Thangaraju M, Prasad P, Ganapathy V, Smith SB (2007) Prevention of excitotoxicity in primary retinal ganglion cells by (+)-pentazocine, a sigma receptor-1 specific ligand. *Invest Ophthalmol Vis Sci* 48(10):4785–4794.
20. Cantarella G, et al. (2007) Protective effects of the sigma agonist Pre-084 in the rat retina. *Br J Ophthalmol* 91(10):1382–1384.
21. Smith SB, et al. (2008) In vivo protection against retinal neurodegeneration by sigma receptor 1 ligand (+)-pentazocine. *Invest Ophthalmol Vis Sci* 49(9):4154–4161.
22. Walker JM, et al. (1990) Sigma receptors: Biology and function. *Pharmacol Rev* 42(4): 355–402.
23. Ha Y, et al. (2011) Sigma receptor 1 modulates endoplasmic reticulum stress in retinal neurons. *Invest Ophthalmol Vis Sci* 52(1):527–540.
24. Mueller BH, 2nd, et al. (2013) Sigma-1 receptor stimulation attenuates calcium influx through activated L-type Voltage Gated Calcium Channels in purified retinal ganglion cells. *Exp Eye Res* 107:21–31.
25. Ha Y, et al. (2014) Sigma receptor 1 modulates ER stress and Bcl2 in murine retina. *Cell Tissue Res* 356(1):15–27.
26. Tchedre KT, et al. (2008) Sigma-1 receptor regulation of voltage-gated calcium channels involves a direct interaction. *Invest Ophthalmol Vis Sci* 49(11):4993–5002.
27. Ha Y, et al. (2011) Late-onset inner retinal dysfunction in mice lacking sigma receptor 1 (σR1). *Invest Ophthalmol Vis Sci* 52(10):7749–7760.
28. Mavlyutov TA, Nickells RW, Guo LW (2011) Accelerated retinal ganglion cell death in mice deficient in the Sigma-1 receptor. *Mol Vis* 17:1034–1043.
29. Ha Y, et al. (2012) Diabetes accelerates retinal ganglion cell dysfunction in mice lacking sigma receptor 1. *Mol Vis* 18:2860–2870.
30. Wang J, Cui X, Roon P, Smith SB (2016) Role of Sigma 1 Receptor in retinal degeneration of the *Ins2*$^{Akita/+}$ murine model of diabetic retinopathy. *Invest Ophthalmol Vis Sci* 57(6):2770–2781.
31. Wang J, et al. (2015) Sigma 1 receptor regulates the oxidative stress response in primary retinal Müller glial cells via NRF2 signaling and system xc(-), the Na(+)-independent glutamate-cystine exchanger. *Free Radic Biol Med* 86:25–36.
32. Mori T, Hayashi T, Hayashi E, Su TP (2013) Sigma-1 receptor chaperone at the ER-mitochondrion interface mediates the mitochondrion-ER-nucleus signaling for cellular survival. *PLoS One* 8(10):e76941.
33. Wang L, et al. (2012) Sigma 1 receptor stimulation protects against oxidative damage through suppression of the ER stress responses in the human lens. *Mech Ageing Dev* 133(11-12):665–674.
34. Pal A, et al. (2012) The sigma-1 receptor protects against cellular oxidative stress and activates antioxidant response elements. *Eur J Pharmacol* 682(1-3):12–20.
35. Zhao J, et al. (2014) Sigma receptor ligand, (+)-pentazocine, suppresses inflammatory responses of retinal microglia. *Invest Ophthalmol Vis Sci* 55(6):3375–3384.
36. Campochiaro PA, et al. (2015) Is there excess oxidative stress and damage in eyes of patients with retinitis pigmentosa? *Antioxid Redox Signal* 23(7):643–648.
37. Johnson DA, Johnson JA (2015) Nrf2–a therapeutic target for the treatment of neurodegenerative diseases. *Free Radic Biol Med* 88(Pt B):253–267.
38. Canning P, Sorrell FJ, Bullock AN (2015) Structural basis of Keap1 interactions with Nrf2. *Free Radic Biol Med* 88(Pt B):101–107.
39. Xiong W, MacColl Garfinkel AE, Li Y, Benowitz LI, Cepko CL (2015) NRF2 promotes neuronal survival in neurodegeneration and acute nerve damage. *J Clin Invest* 125(4): 1433–1445.
40. Gargini C, Terzibasi E, Mazzoni F, Strettoi E (2007) Retinal organization in the retinal degeneration 10 (rd10) mutant mouse: A morphological and ERG study. *J Comp Neurol* 500(2):222–238.

PNAS PLUS
NEUROSCIENCE
Downloaded by guest on February 24, 2022

41. Barhoum R, et al. (2008) Functional and structural modifications during retinal degeneration in the rd10 mouse. *Neuroscience* 155(3):698–713.
42. Phillips MJ, Otteson DC, Sherry DM (2010) Progression of neuronal and synaptic remodeling in the rd10 mouse model of retinitis pigmentosa. *J Comp Neurol* 518(11): 2071–2089.
43. Bringmann A, Wiedemann P (2012) Müller glial cells in retinal disease. *Ophthalmologica* 227(1):1–19.
44. Karlstetter M, et al. (2015) Retinal microglia: Just bystander or target for therapy? *Prog Retin Eye Res* 45:30–57.
45. Usui S, et al. (2011) Overexpression of SOD in retina: Need for increase in H2O2-detoxifying enzyme in same cellular compartment. *Free Radic Biol Med* 51(7):1347–1354.
46. Obolensky A, et al. (2011) Zinc-desferrioxamine attenuates retinal degeneration in the rd10 mouse model of retinitis pigmentosa. *Free Radic Biol Med* 51(8):1482–1491.
47. Shimazawa M, Sugitani S, Inoue Y, Tsuruma K, Hara H (2015) Effect of a sigma-1 receptor agonist, cutamesine dihydrochloride (SA4503), on photoreceptor cell death against light-induced damage. *Exp Eye Res* 132:64–72.
48. Zhao J, et al. (2016) (+)-Pentazocine Reduces NMDA-Induced Murine Retinal Ganglion Cell Death Through a σR1-Dependent Mechanism. *Invest Ophthalmol Vis Sci* 57(2): 453–461.
49. Ola MS, et al. (2001) Expression pattern of sigma receptor 1 mRNA and protein in mammalian retina. *Brain Res Mol Brain Res* 95(1-2):86–95.
50. Jiang G, et al. (2006) Expression, subcellular localization, and regulation of sigma receptor in retinal muller cells. *Invest Ophthalmol Vis Sci* 47(12):5576–5582.
51. Mavlyutov TA, Epstein M, Guo LW (2015) Subcellular localization of the sigma-1 receptor in retinal neurons - an electron microscopy study. *Sci Rep* 5:10689.
52. Huang C, et al. (2015) Activation of the UPR protects against cigarette smoke-induced RPE apoptosis through up-regulation of Nrf2. *J Biol Chem* 290(9):5367–5380.
53. Doonan F, O'Driscoll C, Kenna P, Cotter TG (2011) Enhancing survival of photoreceptor cells in vivo using the synthetic progestin Norgestrel. *J Neurochem* 118(5): 915–927.
54. Usui S, et al. (2009) Increased expression of catalase and superoxide dismutase 2 reduces cone cell death in retinitis pigmentosa. *Mol Ther* 17(5):778–786.
55. Lee SY, et al. (2011) N-Acetylcysteine promotes long-term survival of cones in a model of retinitis pigmentosa. *J Cell Physiol* 226(7):1843–1849.
56. Zhao L, et al. (2015) Microglial phagocytosis of living photoreceptors contributes to inherited retinal degeneration. *EMBO Mol Med* 7(9):1179–1197.
57. Zacny JP, Hill JL, Black ML, Sadeghi P (1998) Comparing the subjective, psychomotor and physiological effects of intravenous pentazocine and morphine in normal volunteers. *J Pharmacol Exp Ther* 286(3):1197–1207.
58. Chang B, et al. (2007) Two mouse retinal degenerations caused by missense mutations in the beta-subunit of rod cGMP phosphodiesterase gene. *Vision Res* 47(5):624–633.
59. Sabino V, Cottone P, Parylak SL, Steardo L, Zorrilla EP (2009) Sigma-1 receptor knockout mice display a depressive-like phenotype. *Behav Brain Res* 198(2):472–476.
60. Markand S, et al. (2015) Retinal ganglion cell loss and mild vasculopathy in methylene tetrahydrofolate reductase (Mthfr)-deficient mice: A model of mild hyperhomocysteinemia. *Invest Ophthalmol Vis Sci* 56(4):2684–2695.
61. Tawfik A, et al. (2014) Alterations of retinal vasculature in cystathionine-β-synthase heterozygous mice: A model of mild to moderate hyperhomocysteinemia. *Am J Pathol* 184(9):2573–2585.

Downloaded by guest on February 24, 2022